

Scaling of stress drop with recurrence interval and loading velocity for laboratory-derived fault strength relations

Changrong He

Institute of Geology and Laboratory of Tectonophysics, China Seismological Bureau, Beijing, China

Teng-fong Wong

Department of Geosciences, State University of New York at Stony Brook, Stony Brook, USA

Nick M. Beeler

U.S. Geological Survey, Menlo Park, California, USA

Received 22 March 2002; revised 22 October 2002; accepted 4 November 2002; published 23 January 2003.

[1] The dynamics of a spring-slider system with a single degree of freedom was investigated, focusing on two different rate- and state-dependent friction laws. While the inertia-controlled behavior and stick-slip cycles for a system that obeys the slip law have been extensively simulated, this study presents a comparative study of a system that obeys the slowness law. A key conclusion is that for both friction laws the overall stress drops are linearly related to the logarithm of the loading velocity (and the recurrence time) through the velocity-weakening parameter $b - a$ and normal stress. Relatively higher peak stresses, larger quasi-static stress drop, and larger effective fracture energy are associated with a system that obeys the slowness law. Consequently, the partitioning of stress drop between quasi-static and dynamic slips, as well as dynamic overshoot and strength recovery, varies according to whether the slowness or slip law has been adopted. Analytic approximations were derived that elucidate the interplay of dynamics, energetics, and frictional constitutive behavior in controlling the scaling of stress drops with loading velocity and recurrence time. Seismological implications of the scaling behavior are also discussed. *INDEX TERMS*: 3220 Mathematical Geophysics: Nonlinear dynamics; 5104 Physical Properties of Rocks: Fracture and flow; 7209 Seismology: Earthquake dynamics and mechanics; *KEYWORDS*: friction, constitutive equation, stress drop, recurrence time, loading rate, stick-slip

Citation: He, C., T.-f. Wong, and N. M. Beeler, Scaling of stress drop with recurrence interval and loading velocity for laboratory-derived fault strength relations, *J. Geophys. Res.*, 108(B1), 2037, doi:10.1029/2002JB001890, 2003.

1. Introduction

[2] Earthquakes and deformation along natural faults involve the complex interplay of boundary conditions of loading and mechanical response of a highly heterogeneous structure. Physical models are useful in understanding the mechanics of earthquake rupture and in isolating the effects of competing natural mechanisms [Rice, 1983; Rudnicki, 1988; Scholz, 1990]. Even simple models can be helpful in many circumstances, provided that the appropriate physics and mechanics are contained within them and their limitations are kept in mind. A notable example is the single degree of freedom spring-slider model that has provided important insights into triggered earthquake phenomena [Rice and Gu, 1983], nucleation of earthquake slip [Dieterich, 1986], earthquake afterslip [Marone et al., 1991], heterogeneity of fault slip [Boatwright and Cocco, 1996], and dynamics of stick-slip cycle [Rice and Tse, 1986; Cao and Aki, 1986].

[3] The nonlinear dynamics of a spring-slider system hinges on the friction constitutive law that has been prescribed for the sliding surface. In recent years, two classes of rate- and state-dependent friction law are commonly used. When normal stress is constant, one of the friction laws uses state variables that evolve only with slip, whereas the other can also describe evolution with stationary contact time. Accordingly the former is commonly referred to as the “slip law” and the latter as the “slowness law” [Beeler and Tullis, 1994; Perrin et al., 1995; Nakatani and Mochizuki, 1996]. These laws can be extended to explicitly describe the effect of normal stress [Linker and Dieterich, 1992; Dieterich and Linker, 1992].

[4] As far as the frictional responses to velocity changes in quasi-static tests are concerned, most data can be fitted reasonably by either the slip or slowness law. Nevertheless, the two laws also have subtle differences in other aspects. Experimental observations of Beeler and Tullis [1994] indicated that strength changes during slide-hold-slide tests are in better agreement with the slowness law than the slip law. Direct observations of frictional contact by Dieterich and Kilgore [1994, 1996] also show that contact area increases with stationary contact time, a phenomenon that

the slip law can not capture. In their continuum dynamics modeling of earthquake rupture as self-healing pulses as proposed by *Heaton* [1990], *Perrin et al.* [1995] concluded that steady pulse solution exists for the slowness law but not for slip law.

[5] Previous analyses of nonlinear dynamics of the spring-slider system have focused on the slip law [e.g., *Rice and Tse*, 1986; *Cao and Aki*, 1986; *Gu and Wong*, 1991; *Weeks*, 1993; *Boatwright and Cocco*, 1996]. Likewise investigations of the dynamics under variable normal stress [*He et al.*, 1998] have been conducted for the slip law only. While linear stability analyses [*Ruina*, 1983] have shown that the slip and slowness laws give identical responses under small perturbations, *Ranjith and Rice* [1999] recently showed that nonlinear stability behavior for the slowness law can be very different from that for the slip law [*Gu et al.*, 1984]. Therefore, it is likely that the inertia-controlled motion in a stick-slip cycle will also have different dynamic attributes for the two classes of friction law.

[6] In this study, we investigate systematically the dynamics of stick-slip cycles in a spring-slider system that obeys the slowness law, with several questions specifically in mind. To our knowledge, the influence of inertia on such a system has not been investigated systematically. Previous studies on the slip law [e.g., *Cao and Aki*, 1986; *Gu and Wong*, 1991] have shown that the stress drops increase with decreasing loading velocity and increasing recurrence time. How are the dynamic attributes (such as the dynamic and static stress drops, dynamic overshoot, and recurrence time) different from those in a system obeying the slip law? *Gu and Wong* [1991] have demonstrated that the dynamic and static stress drops scale with the velocity-weakening parameter $b - a$ in a system obeying the slip law, and yet *Marone's* [1998] quasi-static approximation suggests that the static stress drop scales with the evolution parameter b instead in a system obeying the slowness law. Does this apparent discrepancy represent intrinsic differences between the dynamic responses of systems obeying the two different friction laws? The scaling relations have been established empirically by numerical simulations. Can these relations be interpreted by basic considerations of the mechanics and energetics of the spring-slider system? *Ben-Zion and Rice's* [1997] dynamic simulation of slip on a smooth fault embedded in an elastic solid showed that the dynamic overshoot is higher if friction evolves according to the slip law. Is such dynamic behavior in a continuum model also observed in a spring-slider system?

[7] To address these questions, the present work studies the characteristics of dynamic motion of a single degree of freedom spring-slider system under conditions of constant normal stress, focusing on the slowness law. To elucidate the subtle differences between the two evolution laws, the new simulations are compared with previous studies for the slip law. General scaling relations that may be applicable to a system obeying a rate- and state-dependent friction law are summarized, and seismological implications will also be discussed.

2. Friction Constitutive Equations

[8] For frictional sliding following a rate- and state-dependent law, the shear stress τ is related to normal stress

σ , slip velocity V , and state variable θ as follows [*Linker and Dieterich*, 1992]

$$\tau = \mu_* \sigma + a \sigma \ln(V/V_*) + b \sigma \ln(\theta/\theta_*) \quad (1)$$

where μ_* and θ_* denote steady state values of the friction coefficient and state variable at the reference velocity V_* . For the slowness law the evolution of the state variable (under constant normal stress) is governed by the following differential equation,

$$\frac{d\theta}{dt} = 1 - \frac{\theta V}{D_c} \quad (2a)$$

where D_c is a characteristic distance for the evolution of frictional strength. It can be seen from (2a) that the state variable increases linearly with time when the frictional surface is under stationary contact (with slip velocity $V = 0$).

[9] For the slip law the evolution of state variable is described by the following equation [*Linker and Dieterich*, 1992]:

$$\frac{d\theta}{dt} = -\frac{V\theta}{D_c} \ln\left(\frac{V\theta}{D_c}\right) \quad (2b)$$

It should be noted that the evolution of the state variable is quite different for slip velocities approaching zero. (2b) implicitly rules out the possibility of stationary contact, and the state variable can evolve only if slip occurs under nonzero velocity [*Ruina*, 1983].

[10] Notwithstanding this difference, the two evolution laws (2a) and (2b) have several common features. First, under steady state the state variable is a constant given by $\theta_{ss} = D_c/V$, and in particular $\theta_* = D_c/V_*$. Second, the steady state frictional strength (on substituting into (1)) is $\tau_{ss} = \mu_* \sigma + (a - b)\sigma \ln(V/V_*)$ for both evolution laws.

[11] Before moving on to discuss numerical simulation, some notational differences in the literature should be noted. For the state variable, we have followed the study of *Linker and Dieterich* [1992] to define θ as a quantity with the dimension of time. In many previous studies dealing with the slip law [e.g., *Gu et al.*, 1984; *Rice and Tse*, 1986; *Gu and Wong*, 1991; *Boatwright and Cocco*, 1996; *He et al.*, 1998] a nondimensional state variable of the form $\Theta = b \ln(V_* \theta / D_c)$ is used instead. Furthermore we have used the nondimensional forms (a and b) of the frictional constitutive parameters and denoted the characteristic length by D_c . In a number of previous studies [e.g., *Gu et al.*, 1984; *Rice and Tse*, 1986; *Gu and Wong*, 1991; *Boatwright and Cocco*, 1996; *Ranjith and Rice*, 1999], the characteristic length is denoted by L , and the constitutive parameters ($A = \sigma a$ and $B = \sigma b$) have dimensions of stress.

3. Dynamics of Spring-Slider System Under Constant Normal Stress

[12] We consider the dynamics of a spring-slider system with a single degree of freedom (Figure 1). The slider has unit area and mass m , and the stiffness (spring constant) is k . The spring applies a force on the slider which is proportional to the displacement of the slider δ relative to that of

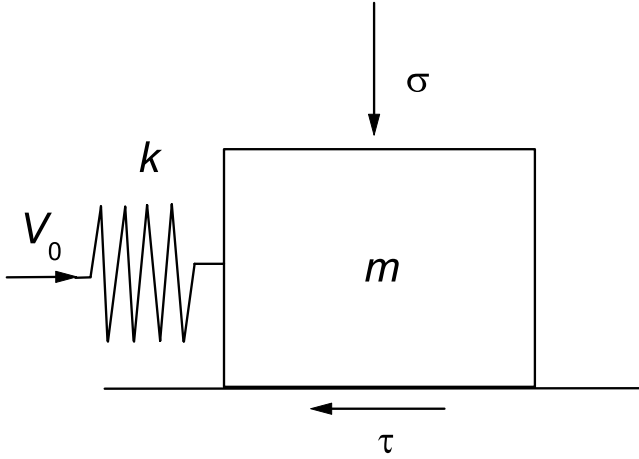


Figure 1. A spring-slider system with single degree of freedom. The slider has unit area and mass m , and the spring constant is k . Constant normal stress σ is applied.

the load point δ_o , and the slider moves when this spring force overcomes the frictional resistance τ . The equation of motion of this system is therefore

$$m \frac{d^2 \delta}{dt^2} = k(\delta_o - \delta) - \tau \quad (3)$$

where time is denoted by t . The slip velocity will be denoted by $V = d\delta/dt$. Combining (1) and (3) and either (2a) or (2b), we obtain a system of ordinary differential equations that govern the dynamics of the spring-slider system obeying the specific friction law. Linear stability analyses have shown that the critical stiffness for both evolution laws is given by $k_{cr} = \sigma(b - a)/D_c$. If the stiffness is lower than this critical value, the spring-slider system will undergo stick-slip cycles when loaded at a constant load point velocity $V_o = d\delta_o/dt$. The mathematical analysis is simplified by normalizations suggested by *Gu et al.* [1984] and *Ranjith and Rice* [1999] for the slip law and slowness law, respectively, and the numerical procedure adopted here is identical to that of *He and Ma* [1997] and *He et al.* [1998].

3.1. Stick-Slip Cycles: Slip Versus Slowness

[13] The development of cyclic stick-slip for the slowness law is illustrated in stress-velocity phase plane for the case of $b/a = 2$, $k/k_{cr} = k/[\sigma(b - a)/D_c] = 0.8$, and $T = 2\pi\sqrt{m/k} = 5s$ (Figure 2). For comparison, the simulation using the slip law for the same parameters are also included. The stick-slip cycles are qualitatively similar. The peak stress is attained at the point A, beyond which the slip velocity increases rapidly. At point B, the sliding motion undergoes a transition from being quasi-static to dominated by inertia. This transition is manifested by the velocity V increasing to above a threshold, which in our simulations is defined by the criterion $2\pi D_c/(VT) < 5 \times 10^{-4}$. Once this threshold velocity has been attained the left-hand term of (3) cannot be neglected, and the stress drops drastically while the motion accelerates until the velocity attains a maximum at C. At this point the spring force is exactly balanced by the frictional resistance, beyond which the motion decelerates and the stress drops further during this dynamic overshoot. The overshoot ends at point D, which also represents the minimum frictional stress in the stick-slip cycle. The stress

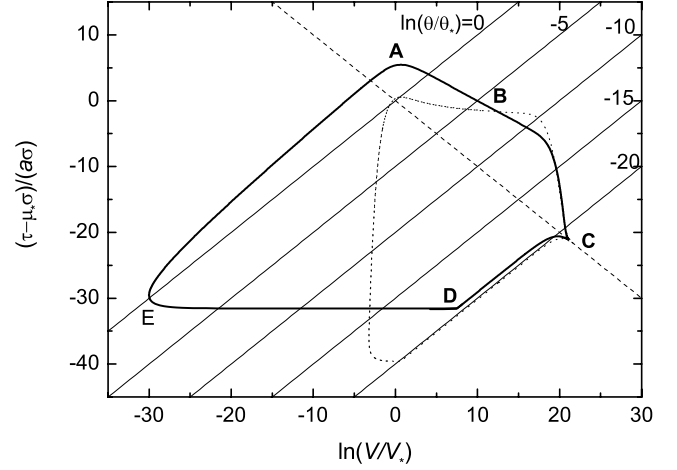


Figure 2. Stress-velocity phase plane plot with $k = 0.8 k_{cr}$, $T = 5$ s, $b/a = 2$, and $V_*/D_c = 1.17 \times 10^{-8} \text{ s}^{-1}$, $V_o = 2V_*$. The limit cycle for a system obeying the slowness law (solid line) is compared with the slip law (dotted line). Steady state line (dashed line) and constant state lines (thin solid lines) are also plotted for reference. For the slowness law case, it should be noted that there is a fast healing process during initial stage of the “stick” phase, which is characterized by the subhorizontal trajectory with drastic decrease (~ 17 orders of magnitude) in slip velocity.

drop process from A to D represents the “slip” phase of the cycle, whereas the subsequent strengthening from D to A represents the “stick” phase that occurs over a significantly longer timescale, that approximately spans the totality of the recurrence time for the stick-slip cycle. The corresponding curves for stress as function of slip are presented in Figure 3.

[14] We have conducted simulations for a range of parameters, with b/a ranging from 1.2 to 2.0, k/k_{cr} ranging from 0.05 to 0.95 and V_o/V_* ranging from 2 to 1024, while keeping T fixed at 5 s (Table 1). While the stick-slip behavior for both evolution laws is qualitatively similar, our simulations show that there are several important differences. (1) For the slowness law, the peak stress increases

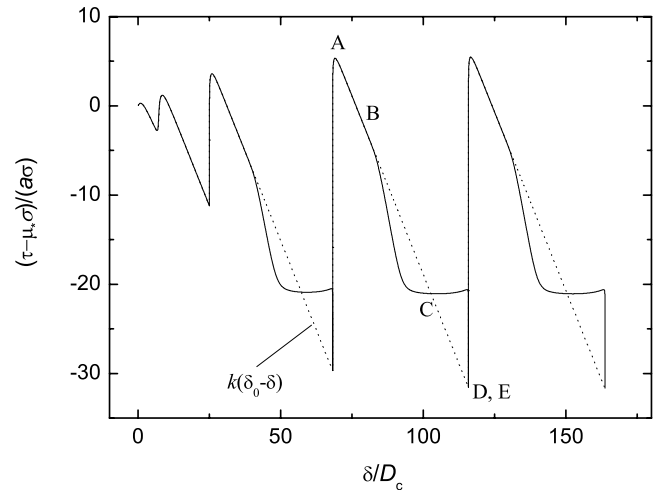


Figure 3. Normalized stress as function of slip for the slowness law case. The last two stick-slip cycles correspond to the limit cycle plotted in Figure 2.

Table 1. Numerical Simulation Data for a System Obeying the Slowness Law

V_o/V_*	$kD_c/\sigma a$	$(b-a)/a$	T (s)	$\ln(V_o/V_*)$	$\Delta t V_*/D_c$	$\Delta \tau_s/\sigma(b-a)$	$\Delta \tau_d/\sigma(b-a)$	$G/D_c(b-a)\sigma$
4	0.05	1	5	24.98	334.94	66.63	33.96	561.0
64	0.05	1	5	24.89	19.06	60.70	30.98	490.2
1024	0.05	1	5	24.79	1.07	54.72	27.97	426.3
4	0.2	1	5	23.39	72.20	56.43	29.80	320.2
64	0.2	1	5	23.29	4.07	51.04	27.03	275.1
1024	0.2	1	5	23.17	0.23	45.57	24.22	237.3
4	0.4	1	5	22.47	31.51	47.64	26.58	235.2
64	0.4	1	5	22.36	1.76	43.11	24.18	209.8
1024	0.4	1	5	22.24	0.10	38.49	21.73	168.5
64	0.95	1	5	20.11	0.45	20.73	15.83	47.3
256	0.95	1	5	20.07	0.11	20.31	15.59	44.1
1024	0.95	1	5	20.02	0.025	19.86	15.33	41.6
4	0.025	0.5	5	25.07	364.60	72.47	36.88	552.8
64	0.025	0.5	5	24.98	20.87	66.43	33.84	491.7
1024	0.025	0.5	5	24.88	1.18	60.32	30.77	436.1
4	0.1	0.5	5	23.48	79.02	61.47	32.29	304.6
64	0.1	0.5	5	23.39	4.48	56.04	29.52	265.9
1024	0.1	0.5	5	23.28	0.25	50.51	26.70	236.5
4	0.2	0.5	5	22.56	34.63	51.86	28.61	219.9
64	0.2	0.5	5	22.47	1.96	47.38	26.29	196.2
1024	0.2	0.5	5	22.36	0.11	42.79	23.91	187.7
16	0.475	0.5	5	20.35	2.15	23.77	17.46	56.7
64	0.475	0.5	5	20.32	0.51	23.40	17.27	52.7
1024	0.475	0.5	5	20.23	0.029	22.51	16.81	48.6
4	0.01	0.2	5	25.25	437.42	86.86	44.06	593.2
16	0.01	0.2	5	25.21	105.30	83.67	42.47	563.8
64	0.01	0.2	5	25.17	25.27	80.45	40.85	542.4
4	0.04	0.2	5	23.68	96.00	74.49	38.76	315.8
64	0.04	0.2	5	23.60	5.51	68.75	35.87	287.7
1024	0.04	0.2	5	23.51	0.31	62.88	32.91	257.1
4	0.08	0.2	5	22.78	42.50	63.43	34.36	234.5
64	0.08	0.2	5	22.70	2.43	58.72	31.97	211.9
1024	0.08	0.2	5	22.61	0.14	53.90	29.53	198.4
64	0.19	0.2	5	20.67	0.66	30.45	21.10	82.9
256	0.19	0.2	5	20.64	0.16	30.06	20.91	79.0

with decreasing loading velocity (Figure 4), following a scaling relation given by

$$(\tau_{\max} - \sigma_{\mu_*})/[\sigma(b-a)] = D - \gamma \ln(V_o/V_*). \quad (4a)$$

with $\gamma \approx 1.1$. The parameter D depends on the mass, stiffness and friction constitutive parameters, but is independent of loading velocity. It ranges from 6.2 to 13.5 for stiffness ratio fixed at $k = 0.8k_{cr}$. For the slip law the scaling relation is relatively simple, with $D \approx 0$ and $\gamma \approx 1.0$ [Gu and Wong, 1991]. In general, a higher peak stress is attained in a system obeying the slowness law for identical friction constitutive parameters (Figure 4a). (2) The quasi-static stress drop (from point A to B in Figure 2) is appreciably higher in a system obeying the slowness law. (3) The dynamic stress drop (from point B to C in Figure 2) as well as the dynamic overshoot (from point C to D in Figure 2) are smaller for the slowness law case. The dynamic stress drop also increases with decreasing loading velocity, following a scaling relation of the form

$$\Delta \tau_d/[\sigma(b-a)] = C' - \xi \ln(V_o/V_*), \quad (4b)$$

where ξ is a constant that decreases with increasing stiffness. It ranges from 0.38 to 0.45 for stiffness ratio

fixed at $k/k_{cr} = 0.8$ (Figure 4b). The intercept C' depends on the stiffness and mass but is independent of the loading velocity. In a system obeying the slip law the dynamic stress drop follows a similar scaling relation but with $\xi \approx 1$, independent of stiffness [Gu and Wong, 1991]. (4) In a system obeying the slowness law, strength recovery during the ‘‘stick’’ phase initially extends to much lower velocities and takes place at almost constant stress over a longer duration (corresponding to the subhorizontal portion from point D to E in Figure 2), and the state variable comes to a value comparable to the steady state value D_c/V_o which implies recovery to the steady state strength at $V = V_o$. Subsequent loading drives the stress to accumulate monotonically along a trajectory with slope comparable to and

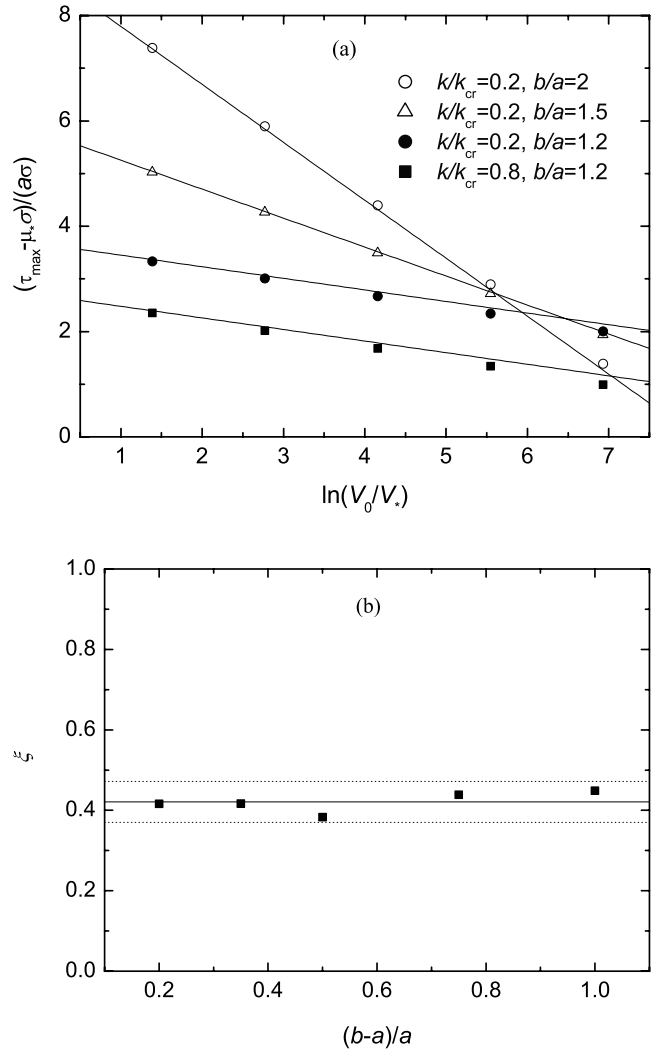


Figure 4. (a) Peak stresses as a function of logarithm of the normalized loading velocity for several sets of stiffness and constitutive parameters. The simulated data fall on linear trends with slopes ranging from 1.08 to 1.2 times $(a-b)/a$, with an average of $\sim 1.1(a-b)/a$, which correspond to the slopes of the thin solid lines. (b) ξ in (4b) as a function of $(b-a)/a$ as stiffness k and mass m are held constant (with $k = 0.8k_{cr}$ and $T = 0.5$ s). The mean value is shown by the solid line, and the dotted lines bracket the mean ± 2 times the standard deviation.

somewhat greater than that of a constant state line, implying further strengthening by a small amount.

3.2. Quasi-Static Stress Drop and Inception of Dynamic Instability

[15] After the peak stress has been attained, the slip velocity increases monotonically while the shear stress drops quasi-statically (from point A to B in Figure 2). According to *Rice and Tse* [1986], the sliding behavior at this stage can be analyzed by neglecting inertia and assuming $V \gg V_0$. For the slowness law, *Ranjith and Rice* [1999, equation (36)] recently obtained an analytic expression for the trajectory of the quasi-static stress drop in the phase plane that can be written as

$$\left(\frac{V}{V_*}\right)^{\frac{(b-a)}{b}} = \frac{k_{cr}}{(k_{cr} - k)} \exp\left\{-\frac{(\tau - \sigma\mu_*)}{\sigma b}\right\} + \frac{Uak_{cr}}{bk} \exp\left\{-\frac{(\tau - \sigma\mu_*)}{\sigma b}\left(1 + \frac{(k_{cr} - k)b}{ka}\right)\right\}, \quad (5a)$$

and for the slip law, *Gu et al.* [1984] derived the following trajectory

$$\frac{(b-a)}{a} \ln\left(\frac{V}{V_*}\right) = \frac{kb}{k_{cr}a} - \frac{(\tau - \sigma\mu_*)}{\sigma a} + P \exp\left\{-\left(\frac{\tau}{\sigma a} \frac{k_{cr}}{k}\right)\right\}. \quad (5b)$$

Appropriate values of the constants U and P are chosen to satisfy the initial conditions. Of interest here are the unstable trajectories, which correspond to positive values of U and P . We compare in Figure 5 these trajectories for the two evolution laws using identical constitutive parameters. It can be seen that the trajectories corresponding to (5a) and (5b) are quite different. For the slip law, a relatively small stress drop occurs quasi-statically since the slip velocity accelerates rapidly (Figure 5b). In contrast, a significant stress drop occurs in the case of the slowness law, for which the quasi-static stress drop is approximately proportional to change in $\ln V$ (Figure 5a). This qualitative difference is reproduced in dynamic simulations of stick-slip cycles, manifested by difference (2b) discussed in the previous section.

[16] That the quasi-static stress drop persists in a system obeying the slowness law is due to the relatively strong resilience of such a system to the development of dynamic instability. A related phenomenon was also noted by *Ranjith and Rice* [1999] in connection with the stability of such a system in response to perturbations in stress or loading velocity. A spring-slider system obeying the slowness law is extremely resilient to perturbations in the sense that dynamic instability is always inhibited, no matter how large a perturbation is imposed as long as the stiffness exceeds the critical value ($k > k_{cr}$). In contrast, instability may arise for sufficiently large perturbations in a system obeying the slip law even if the stiffness exceeds the critical value [*Gu et al.*, 1984]. A reviewer also pointed out that if we used *Nakatani's* [2001] concept using the parameter $\sigma(\mu_* + b \ln(\theta/\theta_*))$ as a proxy for the strength, then a more explicit explanation is possible if we consider

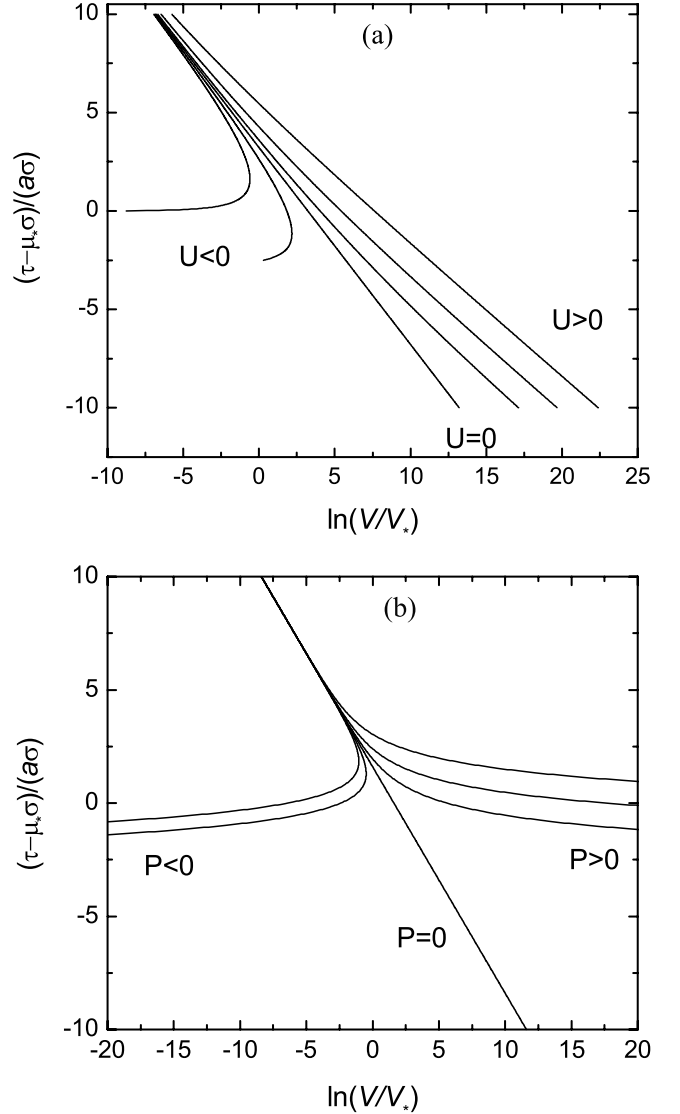


Figure 5. (a) Trajectories for a system obeying the (a) slowness law and (b) slip law when $V_0 \ll V$ (the stationary load point case with $k = 0.8k_{cr}$ and $b/a = 2$) corresponding to (5a) and (5b), respectively.

the evolution of this proxy with slip for the two different friction laws.

4. Scaling of Stress Drops With Loading Velocity and Recurrence Time

4.1. A Spring-Slider System Obeying the Slip Law

[17] The difference in quasi-static drop behavior has implications on the scaling of dynamic and static stress drops. We will first discuss the scaling relations for a system obeying the slip law, for which it has been found that static stress drop is related to the loading velocity and velocity-weakening parameter

$$\frac{\Delta\tau_s}{(b-a)\sigma} = C - \varsigma \ln(V_0/V_*) \quad (6)$$

where $\varsigma \approx 2.0$ and C is a parameter that increases with decreasing stiffness and is independent of loading velocity

[Gu and Wong, 1991]. As noted above, the dynamic stress drop follows the scaling relation (4b) and the peak stress attained in a stick-slip cycle follows the scaling relation (4a).

[18] While Gu and Wong [1991] empirically obtained these relatively simple relations, they failed to come up with a simple mechanical interpretation. With insights gained from our new simulations, we derived analytic approximations for the stress drops that elucidate their dependence on loading velocity, stiffness, and friction constitutive parameters. The mathematical details are presented in Appendix A, and here we summarize the key results.

[19] There are two primary reasons that these simple scaling relations apply to a system obeying the slip law. First, since the quasi-static stress drop is relatively small before the onset of dynamic instability (Figure 2), the quasi-static stress drop can be neglected, and energetic balance can be used to establish the dependence of the dynamic and static stress drops on the loading velocity and stiffness. Second, the mathematical form of the slip law is such that simple scaling relation exists between the phase trajectory and $\ln V_o$ during quasi-static sliding [Gu et al., 1984]. Since the peak stress τ_{\max} is attained during the quasi-static phase, it should also follow this scaling relation.

[20] Reanalyzing Gu and Wong's [1991] simulations, it was found that during the accelerating phase of dynamic instability the slip velocity attains a maximum value that is independent of the loading velocity (but dependent on the spring stiffness, slider mass, and velocity-weakening parameter). This maximum velocity will be denoted by V_L following the study of Rice and Tse [1986], who also noted that the stress τ_L at the termination of the dynamic stress drop is approximately given by the frictional strength for steady state sliding, namely $\tau_L \approx \sigma \mu_* - \sigma(b-a) \ln(V_L/V_*)$. Neglecting the quasi-static stress drop, the dynamic stress drop is then given by $\Delta\tau_d = \tau_{\max} - \tau_L \approx \sigma(b-a) (\ln V_L - \ln V_o)$, which is analogous to (4b) with $C' = \ln(V_L/V_*)$.

[21] During the dynamic slip phase the elastic spring releases strain energy, while dynamic motion of the block is associated with kinetic energy change. In addition, frictional sliding along the surface dissipates an amount of energy equal to $\int \tau d\delta$ integrated over the total dynamic slip. This third energy term can be considered as made up of two parts: the dissipation of energy due to frictional slip at the "residual" level τ_L (equal to the product of τ_L and the total dynamic slip) and an additional component $G = \int (\tau - \tau_L) d\delta$ associated with the dynamic stress drop. In analogy with the slip-weakening models of shear zone and fracture propagation [Rice, 1980; Wong, 1982], we will refer to G as the "effective fracture energy."

[22] If the effective fracture energy G is relatively small, then the energetic balance among the elastic energy, kinetic energy and frictional dissipation requires that total stress drop be partitioned equally between the dynamic stress drop and dynamic overshoot [Rice and Tse, 1986], and therefore the static stress drop (equal to the sum of the dynamic stress drop and overshoot) is simply given by $\Delta\tau_s = 2\Delta\tau_d \approx 2\sigma(b-a) (\ln V_L - \ln V_o)$, which is analogous to (6) with $C = 2\ln(V_L/V_*)$.

[23] A comprehensive series of numerical simulations for a system obeying the slip law were conducted by Gu and Wong [1991], who compiled all their data on stress drops as

functions of loading velocity. However, since they did not include data on maximum velocity and recurrence time, we have included their data in Table 2 for comparison with the analytic approximations. Since they observed that the scaling relations do not seem to apply for constitutive parameters with $(b-a)/a < 0.2$, we have excluded these data in Table 2.

[24] In Appendix A, we also show that energetic considerations allow us to derive analytic estimates of the maximum velocity in terms of the mechanical and constitutive parameters for the slip law. To a first approximation the maximum velocity V_L (and consequently the parameters $C = 2C' = 2\ln(V_L/V_*)$) are independent of the loading velocity V_o , and can be evaluated using (A8): $\ln(V_L/V_*) = -\ln[\sqrt{mk}V_*/(\sigma(b-a))] + \ln\{-\ln[\sqrt{mk}V_*/(\sigma(b-a))]\}$. It is of interest to note that the dimensionless parameter in the analytic approximation can be expressed as $\sqrt{mk}V_*/(\sigma(b-a)) = (k/k_{cr})(T/2\pi)/(D_c/V_*)$, indicating that the stress drops arise from the interplay of the stiffness as well as the dynamic and quasi-static timescales.

[25] In Table 2, we analytically estimate the static stress drop using two different approaches. In the first column (described as "analytic 1"), the stress drop was calculated using $\Delta\tau_s/[\sigma(b-a)] = 2[\ln(V_L) - \ln(V_o)]$ with the maximum velocity values from Gu and Wong's [1991] simulations. In the second column (described as "analytic 2") the stress drop was estimated using (A7) and (A8) using input values of the mass, stiffness and friction constitutive parameters. These two estimates are in satisfactory agreement with the stress drop values from the numerical simulations.

[26] The stress drops are related to loading velocity as well as recurrence time. In a spring-slider model, the system is loaded by the elastic spring at a constant velocity V_o during a stick-slip cycle that recurs over a time interval of Δt . Nearly all of the recurrence time is taken up by the "stick" phase, during which the spring has accumulated a displacement of $\Delta\delta \approx V_o\Delta t$, that corresponds to an elastic stress surplus of $k\Delta\delta \approx kV_o\Delta t$. This surplus is released by frictional slip during the "slip" phase, with strength degradation given by the static stress drop $\Delta\tau_s$. Equating the stress surplus in the spring to static stress drop, the loading velocity and recurrence time are therefore related by $V_o = (\Delta\tau_s/k)\Delta t^{-1}$. If influence of loading velocity on the static stress drop is of second order, then $V_o \propto \Delta t^{-1}$. As elaborated by Beeler et al. [2001], this relation is quite general and seems to apply to a wide range of constitutive behavior.

[27] In Appendix A, we also show that if the influence of loading velocity is taken into account, then we have a scaling relation for the static stress drop in the form of $\Delta\tau_s/[\sigma(b-a)] = \ln(k/(4m)) + 2\ln\Delta t$. Analytic estimates of the static stress drops using this expression are also included as the last column (described as "analytic 3") in Table 2. They are in satisfactory agreement with numerically calculated stress drops.

4.2. A Spring-Slider System Obeying the Slowness Law

[28] We next consider the scaling relations for a system obeying the slowness law. The possibility of stationary contact and strengthening allows such a system to be more resilient to the initiation of dynamic runaway, and as a result

Table 2. Numerical Simulation Data Obtained by *Gu and Wong [1991]*^a

$\frac{V_o}{V_*}$	$\frac{kD_c}{\sigma a}$	$\frac{(b-a)}{a}$	$\frac{M^b}{M_o}$	$\ln\left(\frac{V_L}{V_*}\right)$	$\frac{\Delta V^*}{D_c}$	$\frac{\Delta \tau_s}{\sigma(b-a)}$	Analytic (1)	Analytic (2)	Analytic (3)
0.001	0.8	1	1	21.97	74793.00	53.77	57.75	57.10	58.04
0.001	0.8	1.2	1	22.21	91494.00	57.60	58.23	57.48	58.44
0.1	0.2	0.25	1	20.90	645.80	47.84	46.41	46.42	47.15
0.5	0.8	1	1	21.69	116.68	43.30	44.76	44.67	45.11
1.5	0.05	1	1	23.39	719.27	53.79	45.97	45.39	45.97
1.5	0.267	1	1	22.35	121.87	47.64	43.89	43.63	44.10
1.5	0.667	1	1	21.75	45.18	42.19	42.69	42.66	43.03
1.5	0.727	1	1	21.72	41.24	42.07	42.63	42.57	42.93
1.5	0.8	0.82	1	21.17	28.36	36.49	41.53	42.05	42.28
1.5	0.8	0.9	1	21.44	32.47	39.33	42.08	42.25	42.55
1.5	0.8	1	1	21.63	37.07	40.90	42.45	42.47	42.82
1.5	0.8	1	10,000	16.70	28.91	31.29	32.59	32.69	33.11
1.5	0.8	1	0.5	21.99	37.69	41.55	43.17	43.20	43.54
1.5	0.8	1	0.1	22.85	39.31	43.46	44.89	44.89	45.24
1.5	0.8	1.1	1	21.77	41.31	41.92	42.73	42.67	43.03
1.5	0.8	1.2	1	21.89	45.40	42.54	42.96	42.85	43.22
1.5	0.8	10	1	24.25	412.76	51.00	47.69	47.31	47.64
8	0.2	0.25	1	20.65	6.85	39.72	37.14	37.66	38.05
10	0.8	1	1	21.52	5.09	36.90	38.43	38.68	38.84
10	0.8	1.2	1	21.78	6.21	38.55	38.96	39.06	39.24
20	0.8	1	1	21.48	2.44	35.50	36.96	37.29	37.37
30	0.8	1	1	21.45	1.59	34.80	36.09	36.48	36.52
60	0.8	1	1	21.40	0.76	33.09	34.61	35.09	35.04
100	0.16	0.2	1	20.45	0.51	36.09	31.68	32.37	32.62
100	0.2	0.25	1	20.56	0.48	34.36	31.91	32.61	32.74
100	0.8	1	1	21.37	0.44	32.10	33.52	34.07	33.95
100	0.8	1	10,000	16.35	0.32	22.33	23.49	24.30	24.10
100	0.8	1.2	1	21.64	0.55	33.73	34.07	34.45	34.39
100	0.8	3	1	22.74	1.46	38.05	36.27	36.38	36.35
100	8	10	1	22.67	0.47	35.61	36.13	36.49	36.38
150	0.8	1	1	21.33	0.29	31.36	32.64	33.26	33.11
3000	0.8	1	1	21.07	0.01	24.91	26.13	27.27	26.38

^aThe last three columns are analytical approximations for the normalized static stress drop derived in this study.

^b $M = mV_*^2/(D_c\sigma a)$ and $M_o = 6.9876 \times 10^{-17}$.

the frictional strength attains a higher peak before stress begins to drop and even then it persists to drop in a quasi-static manner for quite a while. Consequently, the scaling of the peak stress (4a) is more complicated for the slowness law and the energetic contribution from quasi-static stress drop cannot be neglected as in the analysis of the slip law.

[29] This complication is also manifested by the relation between static stress drop and recurrence time. In the previous section, we show that if the quasi-static stress drop is negligible then $\Delta\tau_s = kV_o\Delta t$. In Figure 6, we plot our simulation data for the static stress drop versus the product of the loading velocity and recurrence time. It can be seen that except when the stiffness is relatively low, the simulation data deviates from this linear relationship, indicating that the quasi-static contribution cannot be neglected.

[30] To account for the quasi-static stress drop, we observe that its trajectory is approximately linear in the phase plane (Figures 2 and 5a) and we can derive an analytic approximation for the dynamic stress drop based on this feature. The mathematical details are presented in Appendix B. With reference to (4b), the two scaling parameters can be expressed as $\xi = \gamma - \eta$ and $C' = D' + \ln(V_L/V_*)$, where γ is one of the scaling parameters for peak stress in (4a) and D' is related to the other parameter D , and $\eta = (k/k_{cr})/(k/k_{cr} + (b/a)(1 - k/k_{cr}))$. Unlike the slip law case, we cannot analytically derive explicit approximation for V_L .

[31] For the slowness law, our simulations show that the effective fracture energy is generally not negligible (Table 1). The dynamic overshoot $\Delta\tau_{os}$ is smaller than

the dynamic stress drop and can be approximated as $\Delta\tau_{os} = \sqrt{1 - k/k_f}\Delta\tau_d$, where the parameter $k_f \approx b\sigma/D_c$ (Figure 7). The parameters in relation (6) are given by $C = (1 + \sqrt{1 - k/k_f}) [D' + \ln(V_L/V_*)]$ and $\varsigma = (\gamma - \eta)(1 +$

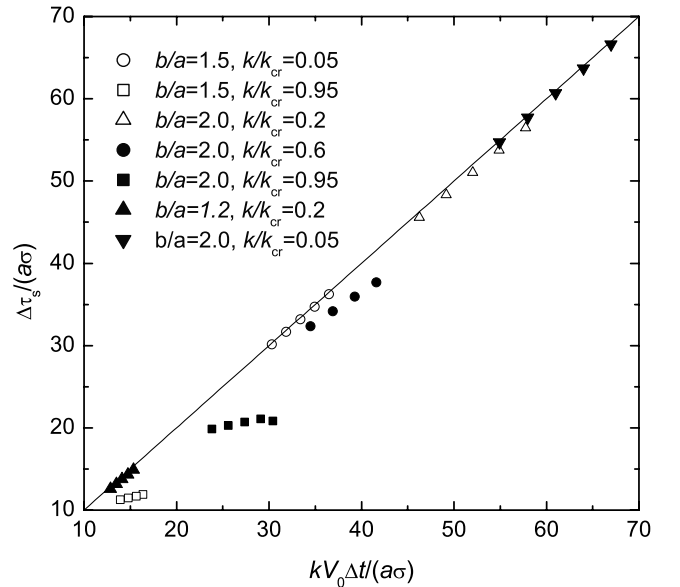


Figure 6. Static stress drops plotted against $kV_o\Delta t$. Data for relatively small stiffnesses fit the relation $\Delta\tau = kV_o\Delta t$, while data for relatively large stiffnesses deviate from this linear relation.

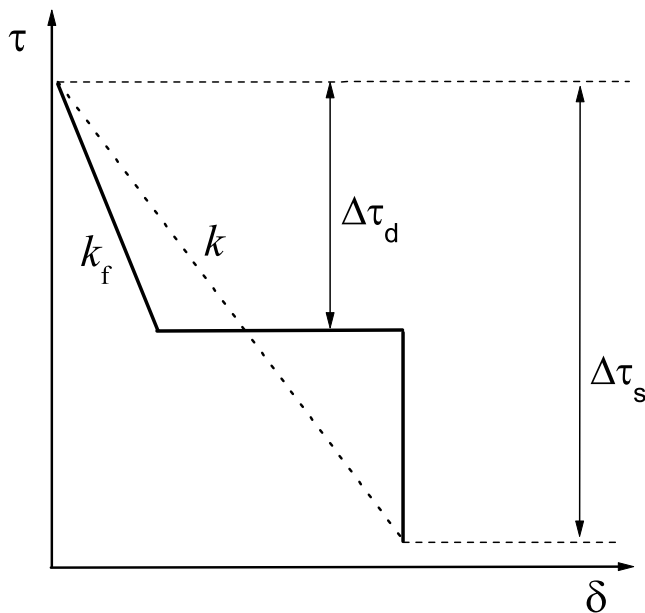


Figure 7. A simplified model showing the relation between static and dynamic stress drops constrained by energy balance. Energetic balance requires that the areas of the upper and lower triangles should be the same.

$\sqrt{1 - k/k_f}$). We note that if $D' \approx 0$, $\gamma \approx 1$, and $k \rightarrow 0$, this scaling of static stress drop for the slowness law is identical to that for the slip law.

[32] Numerical simulations also show a linear relation between static stress drop and logarithm of recurrence time, namely, $\Delta\tau_s/[\sigma(b - a)] = E + \zeta' \ln \Delta t$, similar to the slip law case. The coefficient ζ' is found to be very close to ζ in (6) for the slowness law (Figure 8). This means that approximately $V_o \propto \Delta t^{-1}$ as in the slip law case. In this way, an approximation can also be made by $\zeta' \approx (\gamma - \eta)(1 + \sqrt{1 - k/k_f})$.

5. Discussion

[33] In this study we investigate the nonlinear dynamics of stick-slip in a spring-slider system, focusing on the interplay of elastic loading, friction constitutive relation, and inertia. A key conclusion is that while the details of the partitioning of stress drop between quasi-static and dynamic slips, as well as dynamic overshoot and strength recovery may vary according to the particular evolution law adopted for frictional sliding, the overall stress drops seem to always scale with the loading velocity (and the recurrence time) through the velocity-weakening parameter $b - a$ and normal stress in accordance with (4b) and (6). This type of scaling was empirically established by *Gu and Wong's* [1991] numerical simulations for the slip law, as well as by *Beeler et al.* [2001] who presented preliminary simulations for the slowness law. Here we conduct more systematic simulations that corroborate these preliminary results for the slowness law.

[34] Our simulation data do not support *Marone's* [1998] postulate that stress drops should scale with the loading velocity and recurrence time through the parameter b instead. While his postulate was motivated by a quasi-static

approximation that fails to account for strength recovery during all the phases of an earthquake cycle, our simulations are based on a model that rigorously accounts for inertia and has well-defined boundary conditions and limit cycles. We will discuss first the mechanical interpretation of the dynamical behaviors and their relations to the friction law, and then the seismological implications.

5.1. Mechanical Interpretation of the Nonlinear Dynamics and Scaling Relations

[35] An important feature of a rate- and state-dependent friction law is that it captures the time-dependent healing of the frictional strength. In the context of a stick-slip cycle, this feature allows for the strengthening from the minimum to the maximum friction during the “stick” phase. The two evolution laws analyzed here differ in how they model the healing process in the limit of vanishing slip velocity. Our study underscores how these subtle differences result in qualitatively different responses in the peak stress, quasi-static stress drop and dynamic instability during a stick-slip cycle.

[36] If the frictional surface evolves according to the slowness law, truly stationary contact with zero velocity can be attained. As illustrated in Figure 2, the velocity decreases by a factor of up to e^{40} (i.e., 17 orders of magnitude) during the “stick” phase. The healing at very low velocities seems to be more effective in strengthening the frictional surface. While the mechanics of the spring-slider system constrains the peak stress in a stick-slip cycle to be attained when $V = V_o$, τ_{\max} for the slowness law case (4a) is significantly higher than that in the slip law case (which corresponds approximately to the steady state friction at V_o).

[37] As elucidated by *Ranjith and Rice* [1999], a system that obeys the slowness law is more resilient to the inception of dynamic instability, and our simulations demonstrate that this also results in the quasi-static stress drop being significantly higher. In contrast, the quasi-static stress drop in the slip law case is negligible and further simplifies the

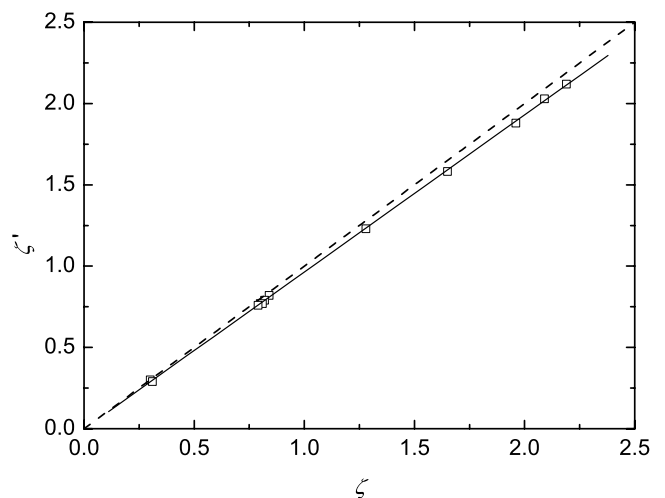


Figure 8. Coefficients ζ' versus ζ in the relation $\Delta\tau/[\sigma(b - a)] = E + \zeta' \ln \Delta t$ and (6), respectively. From linear regression, $\zeta' = 0.966\zeta$ (indicated by the solid line). For reference, the line $\zeta' = \zeta$ is also included as the dashed line.

dynamics. The simpler behavior in this case allows us to analytically approximate the mechanical interaction and energetic balance in a spring-slider system, and explicitly demonstrate in Appendix A how the velocity-weakening parameter $b - a$ enters into the scaling relations (A7) and (A10) for a system obeying the slip law.

[38] While the slowness law introduces additional complications, the analytic approximations presented in Appendix B help quantify their influences on stress drops. After the peak stress has been attained and before inertia becomes important, such a system can sustain a pronounced stress drop while the slider slips quasi-statically (Figures 2 and 3). As a result the dynamic stress drop is relatively small, and its sensitivity to loading velocity is characterized by parameter $\gamma - \eta$ (A13). Physically it represents the trade-off between the time-dependent strengthening enhanced by stationary contact (represented by γ in (4a)) and the quasi-static contribution to stress drop (represented by η in (A11)). Our simulations show that $\gamma - \eta \leq 1$, which agrees with the contention of *Beeler et al.* [2001] that the sensitivity of dynamic stress drop to $\ln V_o$ (and recurrence time Δt) may be weaker than $\sigma(b - a)$, but cannot be as strong as σb , which *Marone* [1998] suggested. Similarly, (A15) and (A16) imply that the sensitivity of the static stress drop may be weaker than $2\sigma(b - a)$.

[39] Our study shows that even though the dynamics is nonlinear, systematic numerical simulations can provide useful insights. It may not be advisable for the sake of mathematical convenience to resort to quasi-static approximation and heuristic choice of loading paths to mimic the dynamics, especially since the nonlinear response is known to be sensitive to subtle changes in the loading path. In this study we have focused on the dynamical behavior under constant normal stress. Both the slip and slowness laws can be extended to explicitly describe the effect of normal stress [*Linker and Dieterich*, 1992; *Dieterich and Linker*, 1992]. Focusing on the slip law, *He and Ma* [1997] and *He et al.* [1998] have analyzed the dynamical behavior of a spring-slider system under variable normal stress, which has notable differences with the constant normal stress scenario. It is of interest to conduct in the future a parallel study of the behavior of such a system that obeys the slowness law.

5.2. Seismological Implications

[40] Both rock mechanics and seismological observations have indicated that stress drops increase with decreasing loading velocity. Some of the first systematic observations in the laboratory were reported by *Wong and Zhao* [1990], who conducted triaxial compression experiments on saw-cut samples sandwiched with ultrafine quartz gouge. Qualitatively similar results were recently reported by *Karner and Marone* [2000] using a biaxial configuration. Using the scaling relation (A7) for the slip law, *Gu and Wong* [1991] showed that *Wong and Zhao's* [1990] data on stick-slip amplitude as a function of loading velocity can be interpreted using $b - a$ values ranging from 0.001 to 0.004, which are comparable to quasi-static measurements in the laboratory. Our simulations here would indicate that the inferred values $b - a$ should be somewhat higher if the slowness law were used to analyze the same data set. While it is of interest to conduct such an analysis, it would require

specific values of additional mechanical parameters of the test machine.

[41] The laboratory data have often been cited to explain why stress drop is found to increase with recurrence interval for some large crustal earthquakes [*Scholz*, 1990]. These seismological observations [*Kanamori and Allen*, 1986; *Scholz et al.*, 1986] suggest that the relative change in static stress drop is large (~ 3 MPa/decade change of recurrence time). Comparable estimates were obtained from more recent studies of stress drop for recurring small earthquakes along the Calaveras fault in Northern California, and repeating events at Parkfield [*Nadeau and McEvilly*, 1999; *Vidale et al.*, 1994].

[42] The comparison between seismological and laboratory data assumes that the room temperature data can be applied directly to frictional sliding at elevated pressures and temperatures at seismogenic depths. Limitations intrinsic to the laboratory and seismological data were reviewed by *Beeler et al.* [2001]. Using scaling relations similar to what we obtain in this study, they considered an example for which $d\Delta\tau_s/d\ln\Delta t \approx 1.37\sigma(b - a)$ with $b - a = 0.002$ (comparable to room temperature laboratory values) and effective normal stress of 18 MPa/km. *Beeler et al.* [2001] concluded that the inferred increase in static stress drop with recurrence ranges from 0.57 to 1.70 MPa/decade, which is toward the low end of seismological estimates.

[43] The implication is therefore that the seismological observations of stress drop increasing with recurrence time cannot be explained by room temperature laboratory mechanisms alone. Similar suggestion have previously been made [*Scholz et al.*, 1986; *Scholz*, 1990; *Gu and Wong*, 1991]. Additional healing mechanisms which may be operative at hydrothermal conditions at seismogenic depths can possibly contribute to the apparent discrepancy between seismic and laboratory data. Deeper understanding of this question would require more systematic investigations of fault strength and frictional behavior under elevated temperatures in the presence of chemically reactive fluids.

6. Conclusion

[44] In the above we presented both numerical and analytical analyses of the behavior of a single degree of freedom spring-slider system that obeys either one of two rate- and state-dependent friction laws. The numerical analyses are mainly focused on the “slowness law” while comparing it with the better-known and mathematically less complicated “slip law.” Before summarizing the results, it should be noted that as far as small perturbations around a certain steady state are concerned, responses for the two laws tend to get close to each other asymptotically as the perturbations decrease. This can be seen from the common critical stiffness obtained by linear analysis for a spring-slider system with the two friction laws [*Ruina*, 1983]. With this and other common features as mentioned in the Introduction in mind, we explored the common features and differences between nonlinear dynamical behaviors due to the two friction laws, and the results are summarized as follows:

1. We have derived explicit analytical approximations for the scaling of stress drop with loading rate, recurrence time,

and friction constitutive parameters for the slip law. The analytic approximations elucidate the control of dynamics, energetics, and frictional behavior on the scaling of stress drops. Similarly for the slowness law which has more complicated behavior, we have obtained implicit relations that clarify the stress drop scaling.

2. As a common feature, systems with both the slip law and slowness law show a negative linear relation between stress drops and logarithm of loading velocity, with coefficients proportional to the velocity-weakening parameter $b - a$. The sensitivity of stress drop to loading velocity is lower for the slowness law.

3. Another common feature is that static stress drop increases linearly with logarithm of recurrence time.

4. While a system with the slip law has peak stress very close to the steady state value corresponding to the loading rate, systems with the slowness law have higher peak stress that scales with loading velocity.

5. For systems that obey the slowness law, stiffness has a strong effect on the sensitivity of stress drop to loading rate. A larger value of stiffness k corresponds to a lower sensitivity. The scaling relations are also complicated because the effective fracture energy cannot be neglected. For a case as $k \rightarrow 0$, the sensitivity of stress drop to loading rate tends to be the same as the slip law.

6. The most remarkable difference between the two friction laws is the development of healing. For the slip law, the state variable recovers mainly during the loading phase, whereas in a system obeying the slowness law the state variable regains most of its value during the early stage of the ‘‘stick’’ phase, when velocity attains a much lower value (decreasing about 17 orders of magnitude) than in the slip law.

Appendix A: Scaling Relations for the Slip Law

[45] There are two primary reasons that the scaling relations for stress drops are relatively simple for a system obeying the slip law. First the quasi-static stress drop is relatively small before the onset of dynamic instability (Figure 2). If the quasi-static stress drop can be neglected, then energetic balance can be conveniently used to establish the dependence of the dynamic and static stress drops on the loading velocity and stiffness. Second, the mathematical form of the slip law is such that a simple scaling relation exists between the phase trajectory and $\ln V_o$ during quasi-static sliding [Gu *et al.*, 1984]. Since the peak stress τ_{\max} is attained during the quasi-static phase, it should also follow this scaling relation.

A1. Energetic Balance During Dynamic Instability

[46] During dynamic instability, the velocity increases to a maximum value V_L (at the point C indicated in Figure 2) with a corresponding stress value of τ_L . For the slip law case the quasi-static stress drop is sufficiently small that we can neglect it, and therefore as a first approximation the dynamic stress drop is simply given by $\Delta\tau_d = \tau_{\max} - \tau_L$, which is accompanied by the release of potential energy $(\Delta\tau_d)^2/(2k) = (\tau_{\max} - \tau_L)^2/(2k)$ in the spring. Since the kinetic energy during quasi-static sliding can be neglected, energetic balance requires that the potential energy is transformed to the kinetic energy $mV_L^2/2$ possessed by the

block at the end of the dynamic instability. Equating the two energies, we arrive at

$$\Delta\tau_d = \tau_{\max} - \tau_L = \sqrt{mk}V_L. \quad (\text{A1})$$

After the maximum velocity has been attained, the slip decelerates and further overshoot in stress drop occurs. If the effective fracture energy is sufficiently small that it can be neglected, then the static stress drop is simply twice the dynamic value [Rice, 1983]

$$\Delta\tau_s = 2\Delta\tau_d = 2(\tau_{\max} - \tau_L) = 2\sqrt{mk}V_L. \quad (\text{A2})$$

[47] To establish the scaling relations for the stress drops, we need to analyze the dependence of τ_{\max} , τ_L and V_L on the loading velocity V_o and recurrence time Δt . For the slip law an elegant result obtained by Gu *et al.* [1984] can be used to analyze the peak stress τ_{\max} . Considering the solution to quasi-static sliding in terms of the dimensionless parameters f , ϕ , T and λ (with $f = (\tau - \tau_*)/(\sigma a)$, $\phi = \ln(V/V_*)$, $T = V_*t/D_c$ and $\lambda = (b - a)/a$), Gu *et al.* [1984] showed that the following scaling rule applies: if $f_1(T)$ and $\phi_1(T)$ are solutions corresponding to a loading velocity V_o , then $f = f_1(sT) - (b - a)/a \ln s$ and $\phi = \phi_1(sT) + \ln s$ is a solution corresponding to the loading velocity sV_o . This scaling rule implies that the quasi-static trajectory for load point V_o will coincide with that for sV_o if we translate the former along a direction parallel to the steady state line (with horizontal shift of $\ln s$ and vertical shift of $-\lambda \ln s$). This behavior is illustrated by Gu and Wong [1991, Figure 4a].

[48] Since the maximum stress is attained during quasi-static sliding, it also follows from this scaling rule that τ_{\max} attained at a faster loading velocity of sV_o is lower than that at V_o by the amount $\sigma(b - a)\ln s$. In other words, the peak stress τ_{\max} should follow the scaling relation $(\tau_{\max} - \sigma\mu_*)/[\sigma(b - a)] = D - \ln(V_o/V_*)$ which was empirically determined by Gu and Wong [1991]. As illustrated by Gu and Wong [1991, Figure 9] (as well as by Rice and Tse [1986, Figure 3a]), the value of D is relatively small such that the peak stress is located in the proximity of the steady state line. Hence to a first approximation $D \approx 0$ and the peak stress is simply given by $\tau_{\max} = \sigma\mu_* - \sigma(b - a)\ln(V_o/V_*)$.

[49] It has also been noted in previous studies that the dynamic instability ends when the phase trajectory intercepts the steady state line [Rice and Tse, 1986], which implies that the stress drops dynamically to the steady state frictional stress value corresponding to the maximum velocity V_L , namely $\tau_L = \sigma\mu_* - \sigma(b - a)\ln(V_L/V_*)$ (Figure 2). In other words, the stress drops can be approximated by

$$\Delta\tau_s = 2\Delta\tau_d = 2(\tau_{\max} - \tau_L) = 2\sigma(b - a)(\ln V_L - \ln V_o). \quad (\text{A3})$$

A2. Analytic Approximation for Scaling Relation Between Stress Drops and Loading Velocity

[50] To derive an explicit expression for the maximum velocity, we equate (A2) and (A3) to arrive at

$$\ln\left(\frac{V_L}{V_*}\right) - \ln\left(\frac{V_o}{V_*}\right) = \frac{\sqrt{mk}V_*}{\sigma(b - a)}\left(\frac{V_L}{V_*}\right). \quad (\text{A4})$$

Since significant acceleration occurs during the dynamic instability we expect that $V_L \gg V_o$. With reference to Table 2 if we consider a sufficiently narrow range of loading velocity V_o such that $V_L \gg V_o$, then the second term on the left-hand side can be neglected. Therefore, an approximate solution for the maximum velocity can be obtained by solving the equation

$$\ln\left(\frac{V_L}{V_*}\right) \approx \frac{\sqrt{mk}V_*}{\sigma(b-a)} \left(\frac{V_L}{V_*}\right). \quad (\text{A5})$$

While this equation can be solved numerically, here we will derive an analytic approximation that elucidates the control of inertia and constitutive parameters over V_L . If we introduce the parameter $\phi_L = \ln(V_L/V_*)$, then (A5) becomes $\phi_L = \left[\frac{\sqrt{mk}V_*}{\sigma(b-a)}\right] \exp(\phi_L)$ and we seek solution in the form of $\phi_L = \xi - \ln\left[\frac{\sqrt{mk}V_*}{\sigma(b-a)}\right]$. This in turn leads us to solve for ξ as a solution of $\xi - \ln\left[\frac{\sqrt{mk}V_*}{\sigma(b-a)}\right] = \exp(\xi)$. Going over simulation results of *Gu and Wong* [1991], we observe that since the first term is $\sim 10\%$ of the second term, we can drop it and seek an approximate solution of $-\ln\left[\frac{\sqrt{mk}V_*}{\sigma(b-a)}\right] = \exp(\xi)$. Therefore an analytic approximation for the maximum velocity is given by

$$\ln\left(\frac{V_L}{V_*}\right) = -\ln\left[\frac{\sqrt{mk}V_*}{\sigma(b-a)}\right] + \ln\left\{-\ln\left[\frac{\sqrt{mk}V_*}{\sigma(b-a)}\right]\right\}. \quad (\text{A6})$$

[51] On substituting (A6) into (A3), we arrive at the scaling relation empirically determined by *Gu and Wong* [1991]

$$\frac{\Delta\tau_s}{\sigma(b-a)} = C - 2 \ln(V_o/V_*). \quad (\text{A7})$$

with the intercept

$$C \approx 2 \ln\left(\frac{V_L}{V_*}\right) = 2 \left\{ -\ln\left[\frac{\sqrt{mk}V_*}{\sigma(b-a)}\right] + \ln\left(-\ln\left[\frac{\sqrt{mk}V_*}{\sigma(b-a)}\right]\right) \right\}. \quad (\text{A8})$$

[52] In Figure A1, we compare *Gu and Wong*'s [1991] numerical data on maximum velocity (Table 2) with analytic estimates from (A6). It can be seen that the agreement is reasonable, and that the second term in (A6) is almost constant: $\xi = \ln\left\{-\ln\left[\frac{\sqrt{mk}V_*}{\sigma(b-a)}\right]\right\} \approx 3$. The dynamic and static stress drops were plotted as functions of loading velocity by *Gu and Wong* [1991, Figures 11 and 8, respectively].

A3. Analytic Approximations for Scaling Relation Between Stress Drops and Recurrence Time

[53] As *Beeler et al.* [2001] pointed out, the data of *Gu and Wong* [1991] also indicate that the static stress drop for a system obeying the slip law follows a simple scaling relation with respect to the recurrence time Δt

$$\frac{\Delta\tau_s}{\sigma(b-a)} = A + 2 \ln \Delta t \quad (\text{A9})$$

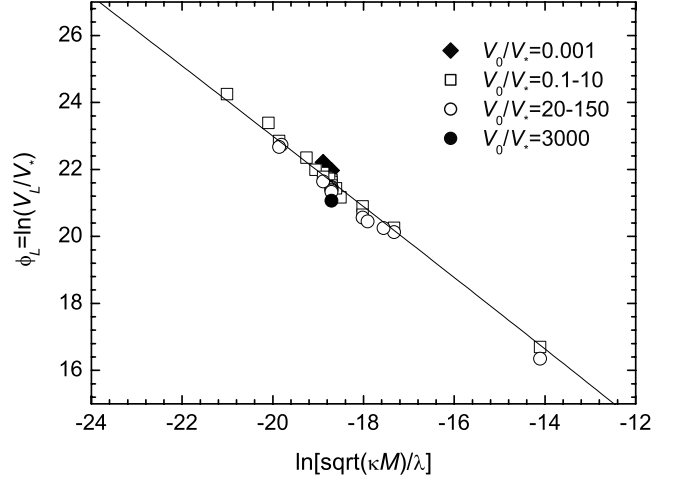


Figure A1. Logarithm of the normalized maximum velocity (V_L/V_*) as a function of logarithm of the normalized parameter $\sqrt{mk}V_*/[\sigma(b-a)]$. The data points are from *Gu and Wong*'s [1991] simulations for different ranges of loading velocity as specified. They are also compiled in the fifth column of Table 2. The continuous line represents the analytic approximation (A6).

This is a manifestation of the strengthening process that is intrinsic to the rate- and state-dependent friction law. Here we will obtain analytic approximation of the intercept A in terms of the mechanical and constitutive parameters of the system.

[54] Let the total displacement accumulated in the spring during the “stick” phase be $\Delta\delta$. The displacement is released by frictional slip that occurs predominantly during the dynamic instability. Again if the effective fracture energy is negligible, then the stress drop as well as the dynamic slip is partitioned equally between the dynamic stress drop and overshoot phases. Using (A1), we therefore have $\Delta\delta/2 \approx \Delta\tau_d/k = \sqrt{m/k}V_L$. In contrast, the total time for a stick-slip cycle is used up mostly by the quasi-static loading at a velocity of V_o . Hence the recurrence time can be estimated as $\Delta t \approx \Delta_d/V_o = 2\sqrt{m/k}V_L/V_o$. Substituting into (A3), we then obtained $\Delta\tau_s = 2\sigma(b-a) \ln\left(\frac{\Delta t}{(2\sqrt{m/k})}\right)$, or equivalently

$$\frac{\Delta\tau_s}{\sigma(b-a)} = \ln\left(\frac{k}{4m}\right) + 2 \ln \Delta t. \quad (\text{A10})$$

Hence the intercept parameter in (A9) can be approximately by $A = \ln(k/(4m))$.

Appendix B: Scaling Relations for the Slowness Law

[55] The scenario for a system that obeys the slowness law is more complicated in two respects. First, even though the governing equation requires that the peak stress of a stick-slip cycle be attained at a slip velocity $V = V_o$, the stress value is somewhat higher than the steady state frictional strength. Our simulations show that $\tau_{\max} = \sigma\mu_* + \sigma(b-a)[D - \gamma \ln(V_o/V_*)]$ with $\gamma \approx 1.1$. Second, appreciable stress drop occurs quasi-statically after the peak stress has been attained. Unlike the slip law case for which

this quasi-static stress drop is negligible, it must be appropriately accounted for in the slowness law case.

B1. Quasi-Static and Dynamic Stress Drops

[56] As illustrated in Figure 2 our simulations for the slowness law show that in the quasi-static phase (from point A to B) the trajectory is approximately linear in the phase plane. Specifically if we consider the normalized parameters $f = (\tau - \tau_*)/(\sigma a)$ and $\phi = \ln(V/V_*)$, the slope of this quasi-static trajectory is approximately given by $df/d\phi = -\eta(b - a)/a$ with

$$\eta = \frac{k/k_{cr}}{k/k_{cr} + (b/a)(1 - k/k_{cr})}. \quad (\text{A11})$$

It can be seen from Figure 5a that the trajectories for $U > 0$ are approximately linear with comparable slopes, and our particular value of $-\eta(b - a)/a$ in (A11) corresponds to the limiting value of the derivative $df/d\phi$ calculated using (5a) at $\phi = 0$ as $U \rightarrow \infty$. Along this quasi-static trajectory, the stress τ at a given slip velocity V is given by $(\tau - \tau_{\max})/(\sigma a) = -\eta[(b - a)/a](\ln V/V_0)$.

[57] Since $\tau_{\max} = \sigma\mu_* + \sigma(b - a)[D - \gamma \ln(V_0/V_*)]$, we can obtain an analytic estimate of the quasi-static stress τ_q before the onset of dynamic instability at a slip velocity V_q

$$\frac{\tau_q - \sigma\mu_*}{\sigma(b - a)} = D - (\gamma - \eta) \ln\left(\frac{V_0}{V_*}\right) - \eta \ln\left(\frac{V_q}{V_*}\right) \quad (\text{A12a})$$

Because V_q is the velocity at which point $T/2\pi \gg Dc/V$, V_q is a constant that depends on D_c , m , and k . Replacing $D - \eta \ln(V_q/V_*)$ with D' , we have

$$\frac{\tau_q - \sigma\mu_*}{\sigma(b - a)} = D' - (\gamma - \eta) \ln\left(\frac{V_0}{V_*}\right) \quad (\text{A12b})$$

With the onset of dynamic instability the stress drops abruptly to the value τ_L , and the dynamic stress drop is given by $\Delta\tau_d = \tau_q - \tau_L$. As noted above the dynamic instability ends when the phase trajectory intercepts the steady state line (Figure 2), which implies that $\tau_L = \sigma\mu_* - \sigma(b - a)\ln(V_L/V_*)$. Combining with (A12b), we obtain

$$\frac{\Delta\tau_d}{\sigma(b - a)} = \frac{\tau_q - \tau_L}{\sigma(b - a)} = D' + \ln\left(\frac{V_L}{V_*}\right) - (\gamma - \eta) \ln\left(\frac{V_0}{V_*}\right), \quad (\text{A13})$$

in a form similar to (4b). We note that if $D' \approx 0$, $\gamma \approx 1$, and $\eta \approx 0$ (corresponding to very small stiffness), (A13) is identical to (A3) derived for the slip law.

[58] As before, we can use energetic balance to determine the maximum velocity. Since the dynamic stress drop releases a potential energy $(\Delta\tau_d)^2/(2k) = (\tau_q - \tau_L)^2/(2k)$ in the spring, energetic balance requires that it is absorbed in part in fracture and is transformed in part to the kinetic energy $mV_L^2/2$ possessed by the block at the end of the dynamic stress drop. From Figure 3, it is seen that most

part of the trajectory during dynamic stress drop is roughly linear. This suggests that the effective fracture energy may be estimated as $(\Delta\tau_d)^2/(2k_f) = (\tau_q - \tau_L)^2/(2k_f)$, with an unloading stiffness $k_f \approx b\sigma/D_C$ as suggested by Dieterich [1994] in an earlier analysis. However, this estimate of G is smaller than the numerical values (compiled in Table 1) by a factor of about 2 due to our ignoring the contribution of the nonlinear part. Empirically we have determined that a better fit is given by $G = (\tau_q - \tau_L)^2/(2k_{fc})$, where the parameter $k_{fc} \approx 0.426 k_f \approx 0.426 b\sigma/D_C$. Considering energetic balance, we arrive at $\Delta\tau_d = \tau_q - \tau_L = \sqrt{mk_{eff}V_L}$, with $k_{eff} = (k_{fc}k)/(k_{fc} - k)$. If we combine this with (A13) and follow arguments similar to those in Appendix A to assume $V_L \gg V_0$, then we arrive at

$$D' + \ln\left(\frac{V_L}{V_*}\right) \approx \frac{\sqrt{mk_{eff}V_*}}{\sigma(b - a)} \left(\frac{V_L}{V_*}\right). \quad (\text{A14})$$

While this equation can be solved numerically, we cannot analytically derive an explicit approximation for V_L in this case.

B2. Static Stress Drop

[59] For the slowness law, our simulations show that the effective fracture energy is generally not negligible and the overshoot is related to the dynamic stress drop by

$$\Delta\tau_{os} = \sqrt{1 - \frac{k}{k_f}} \Delta\tau_d. \quad (\text{A15})$$

where the empirical parameter $k_f \approx b\sigma/D_C$ (Figure 7). We note that if $k \rightarrow 0$ then the potential energy is partitioned equally between the dynamic stress drop and overshoot, but otherwise the dynamic overshoot is smaller than the dynamic stress drop (Figures 2 and 3). Using this result the static stress drop can be estimated as $\Delta\tau_s = \tau_q - \tau_L + \Delta\tau_{os}$, or explicitly as

$$\frac{\Delta\tau_s}{\sigma(b - a)} = \left(D' + \ln\left(\frac{V_L}{V_*}\right)\right) \left\{1 + \sqrt{1 - \frac{k}{k_f}}\right\} - (\gamma - \eta) \left(1 + \sqrt{1 - \frac{k}{k_f}}\right) \ln\left(\frac{V_0}{V_*}\right) \quad (\text{A16})$$

in a form similar to (6). We note that if $\gamma \approx 1$ and $k \rightarrow 0$, sensitivity of stress drop to loading velocity is identical to that in (A3) derived for the slip law.

[60] **Acknowledgments.** We are indebted to Yaojun Gu who conducted the numerical simulations and maintained meticulous records of her extensive data that are compiled in Table 2. We are grateful to Masao Nakatani, John Rudnicki, and Associate Editor Teruo Yamashita for their careful and insightful reviews. The research at China Seismological Bureau was supported by the Ministry of Science and Technology of China under grant G1998040704. The research at Stony Brook was partially supported by the U.S. National Science Foundation under grant EAR-0106580. NMB thanks Steve Hickman of the USGS Western Region Earthquake Hazards Program for support.

References

Beeler, N. M., and T. E. Tullis, The role of time and displacement in the evolution effect in rock friction, *Geophys. Res. Lett.*, 21, 1987–1990, 1994.

- Beeler, N. M., S. H. Hickman, and T.-f. Wong, Earthquake stress drop and laboratory-inferred interseismic strength recovery, *J. Geophys. Res.*, *106*, 30,701–30,713, 2001.
- Ben-Zion, Y., and J. R. Rice, Dynamic simulations of slip on a smooth fault in an elastic solid, *J. Geophys. Res.*, *102*, 17,771–17,784, 1997.
- Boatwright, J., and M. Cocco, Frictional constraints on crustal faulting, *J. Geophys. Res.*, *101*, 13,895–13,909, 1996.
- Cao, T., and K. Aki, Effect of slip rate on stress drop, *Pure Appl. Geophys.*, *124*, 515–529, 1986.
- Dieterich, J., A constitutive law for rate of earthquake production and its application to earthquake clustering, *J. Geophys. Res.*, *99*, 2601–2618, 1994.
- Dieterich, J. H., and B. D. Kilgore, Direct observation of frictional contacts: New insights for state-dependent properties, *Pure Appl. Geophys.*, *143*, 283–302, 1994.
- Dieterich, J. H., and B. D. Kilgore, Imaging surface contacts: Power law contact distributions and contact stresses in quartz, calcite, glass and acrylic plastic, *Tectonophysics*, *256*, 219–239, 1996.
- Dieterich, J. H., and M. F. Linker, Fault stability under conditions of variable normal stress, *Geophys. Res. Lett.*, *19*, 1691–1694, 1992.
- Dieterich, J. H., A model for the nucleation of earthquake slip, in *Earthquake Source Mechanics*, edited by S. Das et al., pp. 37–47, AGU, Washington, D. C., 1986.
- Gu, Y., and T.-F. Wong, Effects of loading velocity, stiffness, and inertia on the dynamics of a single degree of freedom spring-slider system, *J. Geophys. Res.*, *96*, 21,677–21,691, 1991.
- Gu, J.-C., J. R. Rice, A. L. Ruina, and S. T. Tse, Slip motion and stability of a single degree of freedom elastic system with rate and state dependent friction, *J. Mech. Phys. Solids*, *32*, 167–196, 1984.
- He, C., and S. Ma, Dynamic fault motion under variable normal stress condition with rate and state dependent friction, in *Proc. Int. Geol. Congr.*, *30th*, vol. 14, pp. 41–52, VSP, Utrecht, 1997.
- He, C., S. Ma, and J. Huang, Transition between stable sliding and stick-slip due to variation in slip rate under variable normal stress condition, *Geophys. Res. Lett.*, *25*, 3235–3238, 1998.
- Heaton, T. H., Evidence for and implications of self-healing pulses of slip in earthquake rupture, *Phys. Earth Planet. Inter.*, *64*, 1–20, 1990.
- Kanamori, H., and C. R. Allen, Earthquake repeat time and average stress drop, in *Earthquake Source Mechanics*, edited by S. Das, J. Boatwright, and C. H. Scholz, pp. 227–236, AGU, Washington, D. C., 1986.
- Karner, S. L., and C. Marone, Effects of loading rate and normal stress on stress drop and stick-slip recurrence interval, in *Geocomplexity and Physics of Earthquakes*, edited by J. B. Rundle et al., pp. 187–198, AGU, Washington, D. C., 2000.
- Linker, M. F., and J. H. Dieterich, Effects of variable normal stress on rock friction: Observations and constitutive equations, *J. Geophys. Res.*, *97*, 4923–4940, 1992.
- Marone, C., The effect of loading rate on static friction and the rate of fault healing during the earthquake cycle, *Nature*, *391*, 69–72, 1998.
- Marone, C. J., C. H. Scholz, and R. Bilham, On the mechanics of earthquake afterslip, *J. Geophys. Res.*, *96*, 8441–8452, 1991.
- Nadeau, R. M., and T. V. McEvilly, Fault slip rates at depth from recurrence intervals of repeating microearthquakes, *Science*, *285*, 718–721, 1999.
- Nakatani, M., Conceptual and physical clarification of rate and state friction: Frictional sliding as a thermally activated rheology, *J. Geophys. Res.*, *106*, 13,347–13,380, 2001.
- Nakatani, M., and H. Mochizuki, Effect of shear stress applied to surfaces in stationary contact on rock friction, *Geophys. Res. Lett.*, *23*, 869–872, 1996.
- Perrin, G., J. R. Rice, and G. Zheng, Self-healing slip pulse on a frictional surface, *J. Mech. Phys. Solids*, *43*, 1461–1495, 1995.
- Ranjith, K., and J. R. Rice, Stability of quasi-static slip in a single degree of freedom elastic system with rate and state dependent friction, *J. Mech. Phys. Solids*, *47*, 1207–1218, 1999.
- Rice, J. R., The mechanics of earthquake rupture, in *Physics of the Earth's Interior*, edited by A. M. Dziewonski and E. Boschi, pp. 555–649, Ital. Phys. Soc., Bologna, 1980.
- Rice, J. R., Constitutive relations for fault slip and earthquake instabilities, *Pure Appl. Geophys.*, *121*, 443–475, 1983.
- Rice, J. R., and J.-C. Gu, Earthquake aftereffects and triggered seismic phenomena, *Pure Appl. Geophys.*, *121*, 187–219, 1983.
- Rice, J. R., and S. T. Tse, Dynamic motion of a single degree of freedom system following a rate and state dependent friction law, *J. Geophys. Res.*, *91*, 521–530, 1986.
- Rudnicki, J. W., Physical models of earthquake instability and precursory processes, *Pure Appl. Geophys.*, *126*, 531–554, 1988.
- Ruina, A. L., Slip instability and state variable friction laws, *J. Geophys. Res.*, *88*, 10,359–10,370, 1983.
- Scholz, C. H., *The Mechanics of Earthquakes and Faulting*, 433 pp., Cambridge Univ. Press, New York, 1990.
- Scholz, C. H., C. A. Aviles, and S. G. Wesnousky, Scaling differences between large interplate and intraplate earthquakes, *Bull. Seismol. Soc. Am.*, *76*, 65–70, 1986.
- Vidale, J. E., W. L. Ellsworth, A. Cole, and C. Marone, Rupture variation with recurrence interval in 18 cycles of a small earthquake, *Nature*, *368*, 624–626, 1994.
- Weeks, J. D., Constitutive laws for high-velocity frictional sliding and their influence on stress drop during unstable slip, *J. Geophys. Res.*, *98*, 17,637–17,648, 1993.
- Wong, T.-f., Shear fracture energy of westerly granite from post-failure behavior, *J. Geophys. Res.*, *87*, 990–1000, 1982.
- Wong, T.-f., and Y. Zhao, Effects of load point velocity on frictional instability behavior, *Tectonophysics*, *175*, 177–195, 1990.

N. M. Beeler, U.S. Geological Survey, Menlo Park, CA, USA.

C. He, Institute of Geology and Laboratory of Tectonophysics, China Seismological Bureau, China.

T.-f. Wong, Department of Geosciences, State University of New York at Stony Brook, Stony Brook, NY, USA. (Teng-fong.Wong@sunysb.edu)